Journal of Materials Chemistry C

Accepted Manuscript

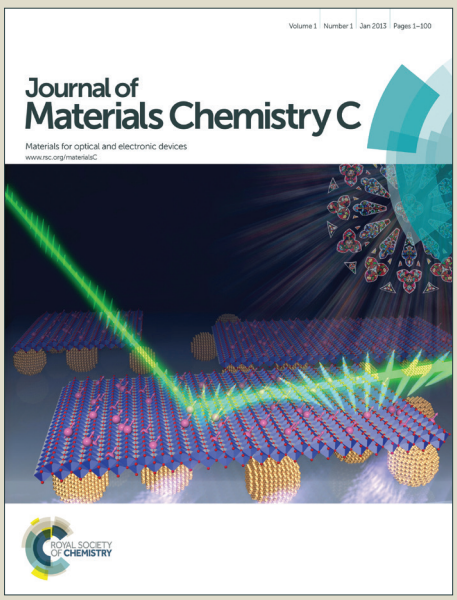

ROYAL SOCIETY OF CHEMISTRY

www.rsc.org/materialsC

Extremely Stable-color Flexible White Organic Light-emitting Diodes with Efficiency Exceeding 100 lm W^{-1}

Baiquan Liu [a)] Lei Wang [a)] Miao Xu [a)] Hong Tao [a)] Dongyu Gao [b)] Jianhua Zou [a)*] Linfeng Lan [a)] Honglong Ning [a)] Junbiao Peng [a)*] Yong Cao [a)]

[a] Institute of Polymer Optoelectronic Materials and Devices, State Key Laboratory of Luminescent Materials and Devices, South China University of Technology, Guangzhou 510640, China

[b] New Vision Opto-Electronic Technology Co., Ltd, Guangzhou 510530, China

Abstract: A flexible white organic light-emitting diode (WOLED) based on a polyethylene naphthalate (PEN) substrate has been developed, simultaneously achieving extremely high efficiency and extremely stable color. By using a superior combination of mechanical, electrical and optical properties, the resultant flexible WOLED can exhibit a maximum forward-viewing PE of 101.3 lm W^{-1}, 77.0 lm W^{-1} at 100 cd m^{-2}, which remains as high as 58.2 lm W^{-1} at 1000 cd m^{-2}. Besides, the device exhibits an excellent color-stability with the Commission International de L'Eclairage variation of (0.004, 0.005) when the luminance increases from 100 cd m^{-2} to 10000 cd m^{-2}. Moreover, the origin of high efficiency and stable color has been comprehensively unveiled. Such presented results provide an effective way to realize high-performance flexible WOLEDs.

Keywords: white organic light-emitting diodes, flexible, efficiency, stable color, outcoupling.

1. Introduction

Organic light-emitting diodes (OLEDs) are now approaching mainstream display markets and also being aggressively explored for the near future lighting applications due to their extraordinary characteristics, such as high efficiency, fast switching and low power consumption.[1-4] To make OLEDs more competitive than other display and lighting counterparts, flexible OLEDs have steadily attracted both scientific and industrial interest owing to their unique merits, including

ultralight weight, small thickness and suitability for roll-to-roll production.[5-21] Heeger et al. took the first step to fabricate a flexible OLED with soluble conducting polymers on a poly(ethylene terephthalate) (PET) substrate.[5] Forrest et al. established the first flexible OLED with small-molecule organic materials.[6] Since then, a large number of attention has been paid to pursue flexible OLEDs. For example, Lu et al. used an efficient anode stack and a lens-based structure to unlock the full potential of a green OLED on flexible plastic, achieving a power efficiency (PE) of 290 lm W^{-1}.[7] Kim et al. combined a low temperature color filter and a microcavity covered with thin film encapsulation, achieving an improved outdoor readability and low power flexible OLED display.[8] Najafabadi et al. constructed a flexible green inverted top-emitting OLED having an outcoupling layer, achieving a current efficiency (CE) of 96.3 cd A^{-1}.[9] Our group has realized China's first full-color flexible active-matrix OLED display[6] and also reported a 5 inch flexible green active-matrix OLED display on a polyethylene naphthalate (PEN) substrate with a process temperature below 150 °C[11].

It is obviously seen that flexible monochromatic OLEDs have been hot research topics in the last few years, and hence, performances are step-by-step enhanced with the concerted efforts of researchers all over the world. Nowadays, flexible white OLEDs (WOLEDs) are of great interest because of the booming market for consumer electronics and large-area lighting applications. For WOLEDs based on glass substrates, performances can satisfy commercial demands in many respects. For instance, the lifetime of WOLEDs with all-flourescent emitters is as long as 150000 h at 1000 cd m^{-2}.[12] The color rendering index (CRI) of WOLEDs is sunlight-like, which is as high as 98.[13] In terms of efficiency, the WOLED without outcoupling technology shows a maximum PE of ~60 lm W^{-1},[14, 15] while the WOLED with outcoupling technologies can potentially exhibit a PE of 124 lm W^{-1}.[16] In the case of flexible WOLEDs, however, efforts have been scarcely taken. Mikami

et al. fabricated a flexible WOLED with a PE of 4.3 lm W^{-1}.[17] Jou et al. realized a flexible WOLED with effective emissive architecture on a modified substrate, achieving a PE of 6.5 lm W^{-1}.[18] Ji et al. prepared a flexible top-emitting WOLED with a CE of 8.66 cd A^{-1}.[19] Han et al. built a two-color WOLED with a multi-layer graphene anode on a PET substrate, achieving a CE of 16.3 cd A^{-1}.[20] Most recently, Li et al. prepared a WOLED with a single-layer graphene anode on a PET substrate, yielding a PE of 90 lm W^{-1} via an outcoupling method combining high index glass substrate with half sphere lens (enhanced by a factor of 3).[21] However, improvements in optical outcoupling that rely on high refractive index substrates are unfavorable to low cost mass production. [7] Besides, half sphere lens are usually only suitable for small-area devices, which are not practical to large-area applications. Moreover, the color-stability, which is a critical parameter to WOLEDs,[22] of these flexible WOLEDs has never been documented. Based on these facts, it can be concluded that the development of flexible WOLEDs is a promising way to meet the rapidly growing requirement of commercialization, however, there is much room to further improve their performances.

In this paper, three strategies are used to develop the extremely high-efficiency and stable-color flexible WOLED. i) Since plastics are the most promising flexible substrate candidates due to lightweight, high transparency and unbreakable nature,[5-21] PEN substrates are selected because they not only exhibit the above merits but also show low cost, full compatibility with thin film transistor process chemistry, moisture pickup, dimensional stability and smoothness.[11, 23, 24] However, despite PEN substrates possess so many advantages, no successful PEN-based WOLED has been reported until now, indicating that an urgent effort needs to be taken. ii) A novel multifunctional carrier- and exciton-confining structure is designed, guaranteeing the high efficiency and stable color. iii) A simplified, low-cost but effective outcoupling approach with suitability for large-area applications is used to free the light trapped by the substrate. With this

unique combination of mechanical, electrical and optical properties, high-performance flexible WOLEDs are developed, as shown in figure 1. The resultant device can exhibit a maximum forward-viewing PE of 101.3 lm W^{-1}, which is the first report that the efficiency of flexible WOLED exceeds 100 lm W^{-1} in the revealed literature so far. The efficiency is 77.0 lm W^{-1} at 100 cd m^{-2}, which remains as high as 58.2 lm W^{-1} at 1000 cd m^{-2}. Besides, the device exhibits an excellent color-stability with the Commission International de L'Eclairage (CIE) variation of (0.004, 0.005) when the luminance increases from 100 cd m^{-2} to 10000 cd m^{-2}. Moreover, the origin of high efficiency and stable color has been comprehensively investigated. Such achieved results provide an effective approach to realize high-performance flexible WOLEDs.

2, Experimental

Figure 1 depicts the studied WOLEDs. The PEN substrate was first attached to the same size glass carrier (conventional alkali-free glass, 0.7 mm thick) during the entire device fabrication process and was separated from the glass only when the device formation was completed. The configuration of flexible WOLEDs is PEN(120 μm)/ITO (170 nm)/MeO-TPD: F4-TCNQ (100 nm,4%)/NPB (15 nm)/TCTA (5 nm)/TCTA: $Ir(dmppy)_2(dpp)$ (1 nm, 20%)/TCTA: FIrpic (4 nm,7%)/26DCzPPy: FIrpic (4 nm, 20%)/26DCzPPy: $Ir(dmppy)_2(dpp)$ (1 nm, 20%)/TmPyPB (50 nm)/LiF (1 nm)/Al (200 nm), where ITO is indium tin oxide (an anode), F4-TCNQ is tetrafluoro-tetracyanoqino dimethane, doped into N, N, N',N'-tetrakis(4-methoxyphenyl)-benzidine (MeO-TPD), NPB is N,N'-di(naphthalene-1-yl)-N,N'-diphenyl-benzidine, TCTA is 4,4',4''-tri(9-carbazoyl) triphenylamine (an exciton/electron blocking layer and a host of orange/blue emitters), $Ir(dmppy)_2(dpp)$ is Bis(2-phenyl-4,5-dimethylpyridinato)[2-(biphenyl-3-yl)pyridinato] iridium(III) (an orange emitter), FIrpic is iridium(III)bis[(4,6-difluo-rophenyl)-pyridinato-N,C2] (a blue emitter),

26DCzPPy is 2,6-bis(3-(carbazol-9-yl)phenyl)pyridine (a host of orange/blue emitters), TmPyPB is 1,3,5-tri(m-pyrid-3-yl-phenyl)benzene, LiF is an electron injection layer and Al is a cathode. Materials were commercially bought and not further purified. All layers were thermally deposited without breaking the vacuum at a base pressure of 2×10^{-7} Torr. Deposition rates of both host and guest were controlled by their correspondingly independent quartz crystal oscillators. Devices were encapsulated immediately after preparation under a nitrogen atmosphere using SiNx(300 nm) thin films which were fabricated at 80 ℃ by PECVD. For the outcoupling film fabrication, the SiO_2 with a refractive index of ~1.5, average particle sizes of 1.5 μm were first dispersed into the SU-8 matrix with a concentration of 15%. By using the blade coating technique, the film thickness was controlled by the gap between the blade and substrate. After drying for 24 h (40 ℃), a 85 μm film was formed. The electroluminescent (EL) spectra, CIE coordinates and CRI of devices were obtained by a Konica Minolta CS2000 spectra system. The emission area of the devices is 5×5 mm^2 as defined by the overlapping area of the anode and cathode. The luminance-current density (J)-voltage (V) characteristics were recorded simultaneously, using a computer-controlled source meter (Keithley 2400) and multimeter (Keithley 2000) with a calibrated silicon photodiode. The lifetime of the devices was tested through a 512 channel OLED testing system (New Vision Opto-Electronic Technology Co., Ltd) at room temperature.

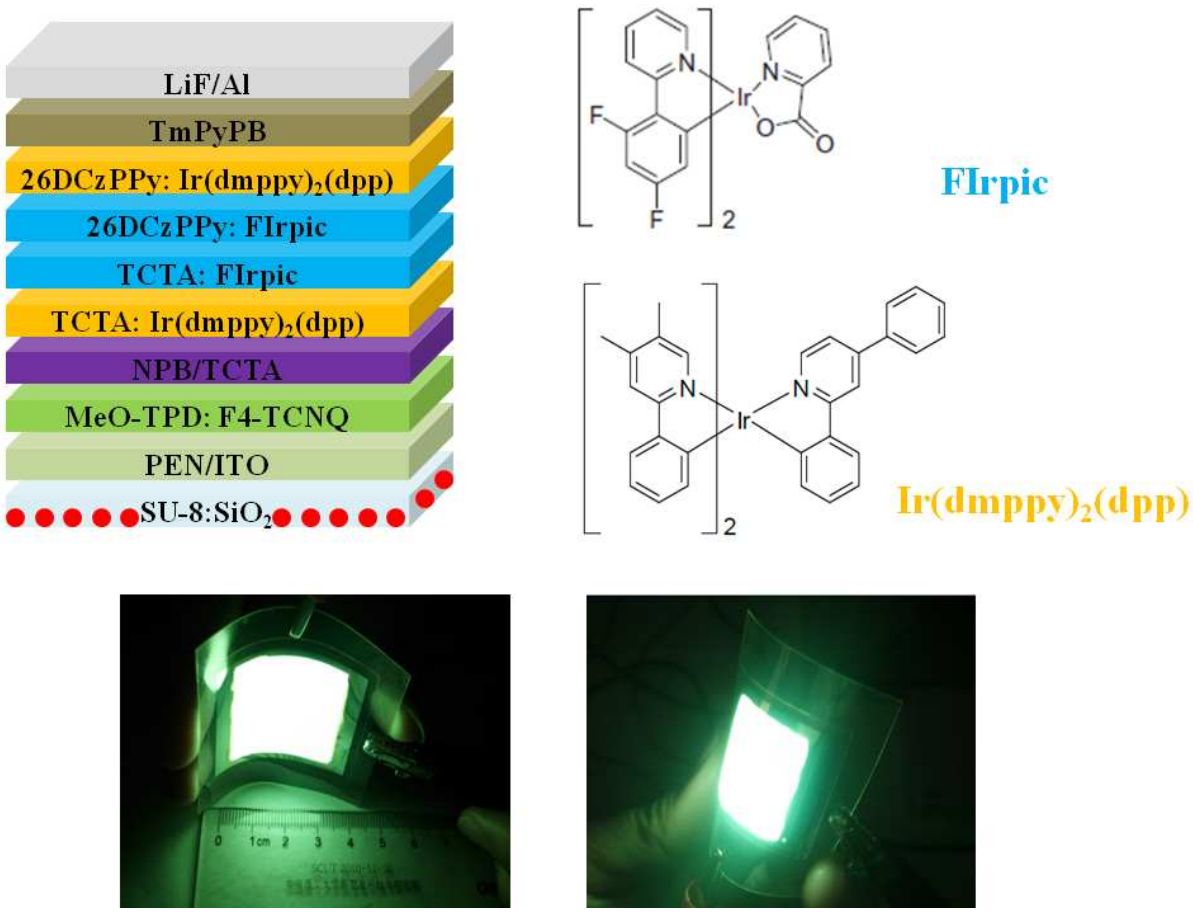

Figure. 1. Top: The schematic structure of WOLEDs and chemical structure of emitters. Bottom: Photographs of large-area flexible WOLEDs (30 mm× 30 mm) working at a high luminance of 1000 cd m^{-2}.

3. Results and discussions

The configuration of device W1 (without outcoupling film) is PEN(120 μm)/ITO (170 nm)/MeO-TPD: F4-TCNQ (100 nm,4%)/NPB (15 nm)/TCTA (5 nm)/TCTA: $Ir(dmppy)_2(dpp)$ (1 nm, 20%)/TCTA: FIrpic (4 nm,7%)/26DCzPPy: FIrpic (4 nm, 20%)/26DCzPPy: $Ir(dmppy)_2(dpp)$ (1 nm, 20%)/TmPyPB (50 nm)/LiF (1 nm)/Al (200 nm), as depicted in figure 1. The forward-viewing CE and PE of W1 in dependence of the luminance are shown in figure 2 and table 1. It is seen that the CE of 58.1 cd A^{-1}, 53.0 cd A^{-1} and 48.7 cd A^{-1} are recorded at 2.5 cd m^{-2}, 100 cd m^{-2} and 1000 cd m^{-2}, respectively. While the PE of 60.4 lm W^{-1}, 46.2 lm W^{-1} and 33.5 lm W^{-1} are

obtained at 2.5 cd m^{-2}, 100 cd m^{-2} and 1000 cd m^{-2}, respectively, representing the highest levels at these typical luminances in flexible WOLEDs without outcoupling technologies. Besides, it is noted that W1 displays lower efficiency roll-off than these representative WOLEDs.[25-28] Remarkably, as illustrated in figure 2 inset, the CIE coordinates of W1 only experience a negligible change from (0.329, 0.463) to (0.328, 0.470) when the luminance increases from 100 cd m^{-2} to 10000 cd m^{-2}, indicating that the device exhibits one of the most stable color among phosphorescent WOLEDs.[29-31]

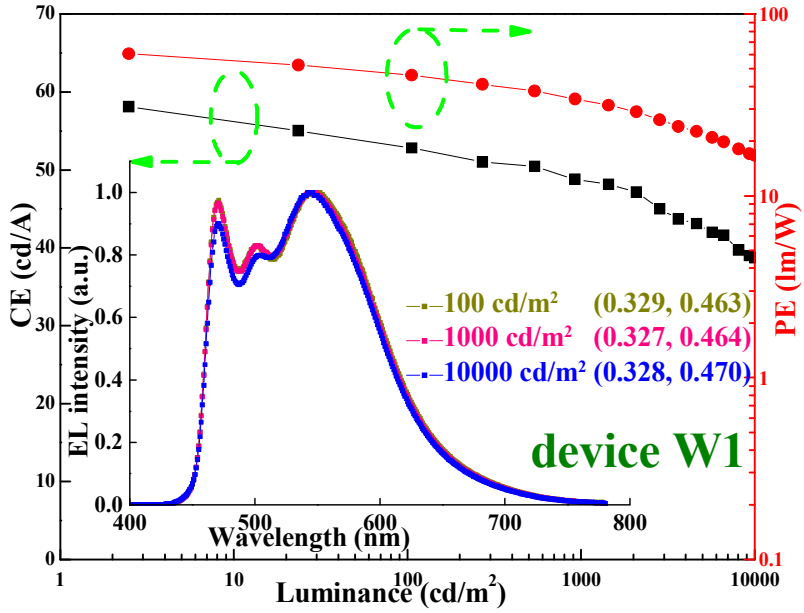

Figure. 2. Current and power efficiencies as a function of luminance for W1. Inset: EL spectrum at various luminances.

Table 1. Performances of flexible WOLEDs.

Device	V_{on} [a] (V)	$CE_{max/100/1000}$ [b] (cd A^{-1})	$PE_{max/100/1000}$ [c] (lm W^{-1})	CIE_{1000} [d]	ΔCIE [e]
W1	3.15	58.1/53.0/48.7	60.4/46.2/33.5	(0.327, 0.464)	(0.002, 0.007)
W2	3.1	96.8/83.8/79.1	101.3/77.0/58.2	(0.319, 0.467)	(0.004, 0.005)

[a] The turn-on voltage (at a luminance of 10 cd/m^2). [b] Maximum CE, CE at 100 cd m^{-2} and CE

at1000 cd m^{-2}. [c] Maximum PE, PE at 100 cd m^{-2} and PE at 1000 cd m^{-2}. [d] CIE at 1000 cd m^{-2}. [e] Total CIE variation during 100- 10000 cd m^{-2}.

Inspired by the outstanding performance of W1, we subsequently performed a comprehensive study to unveil the origin of high efficiency and stable color.

First, desirable host-guest systems are carefully selected and optimized, maximizing exciton formation and emission. As vividly shown in figure 3a, the triplet energy (T_1) of TCTA and 26DCzPPy are 2.76 eV[14] and 2.71 eV[32], respectively, high enough to satisfy FIrpic (2.65 eV)[32] and $Ir(dmppy)_2(dpp)$ (< 2.15 eV)[33], preventing reverse energy transfer from dopants to hosts and confining triplet excitons in the emitting layer (EML), which can consume the triplets contributing to emission[2].

Then, a new device structure is designed to enhance the efficiency. As shown in figure 3a, owing to the existed energy barriers coupled with the fact that TCTA is a p-type material and 26DCzPPy exhibits high electron mobility[32], it can be easily inferred that the main exciton generation zone is located at the TCTA/26DCzPPy interface, which is effectively broadened via the double blue EML[34], reducing the triplet-triplet annihilation and efficiency roll-off [2]. In turn, the reduction in triplet-triplet annihilation can effectively stabilize the color and enhance the efficiency.[22, 34] Moreover, the total thickness of EML is thin (10 nm), which can lower voltages, thus improving efficiency and lowering color-shift.[31] Besides, the orange EMLs are deliberately designed to surround the double blue EML, which can harvest the unused excitons, further enhancing the efficiency. As a result, the orange emission occurred from the combined effects of efficient energy transfer from the blue phosphor and exciton formation by direct charge trapping on $Ir(dmppy)_2(dpp)$ [2, 35]. Hence, it is no wonder that the total orange EML thickness is only 2 nm, a quarter to that of blue EML. This is a key design feature to ensure the efficient white emission,

which is different from Su's structure which inserted ultrathin orange EMLs between the blue EMLs[14] and Leo's concept which needs interlayers to prevent the energy transfer [16].

Next, figure 3a summarizes other reasons for the high efficiency. The p-doped hole injection layer (HIL) [34] and the stepped double hole transport layer (HTL, NPB/TCTA)[15] ensure hole injection, while the lowest unoccupied molecular orbital (LUMO) of TmPyPB (2.7 eV) electron transport layer (ETL)[36] is close to that of 26DCzPPy (2.65 eV)[32] together with the electron mobility of TmPyPB is as high as 10^{-3} cm^2/V s[36], improving electron injection. In contrast, the undoped TCTA blocks electrons,[29] while the deep HOMO of TmPyPB blocks holes. These charge-blocking properties are also important for concentrating charges into the EML, resulting in efficient recombination. Besides, both TCTA and TmPyPB have high singlet energy (S_1) and T_1,[14, 36] greatly confining singlets and triplets in the EML. Therefore, an energetic well-like emitting region is established, charges or excitons are unable to escape upon they falling into this region, increasing the probability that they can radiatively decay from the two emitters. In a word, a versatile carrier- and exciton-confining structure is formed, dramatically boosting the efficiency. [2]

Additionally, the reduction of charge mobility associated with host-dopant energy level difference leads to the recombination ratio being constant in the EML, greatly lowering the color-shift and efficiency roll-off.[2, 30, 31, 37] To clarify the effect of phosphors-doped TCTA and 26DCzPPy on electrical properties, hole-only and electron-only devices were fabricated with configurations of ITO/MeO-TPD : F4-TCNQ (100 nm, 4%)/NPB (15 nm)/TCTA (5 nm)/hosts: dopants (5 nm)/TCTA (20 nm)/Al (200 nm) and ITO/LiF (1 nm)/TmPyPB (50 nm)/hosts: dopants (5 nm)/TmPyPB (50 nm)/LiF (1 nm)/Al (200 nm), respectively, where dopants denote none for H11 and E11, 7% Firpic for H12 and E12, 20% $Ir(dmppy)_2(dpp)$ for H13 and E13 in the TCTA host based devices, and dopants denote none for H21 and E21, 7% FIrpic for H22 and E22, 20%

$Ir(dmppy)_2(dpp)$ for H23 and E23 in the 26DCzPPy host based devices. The J-V curves of these devices exhibit changes for different host-guest systems, as depicted in figure 3b. Comparing H12 or H13 with H11, the hole-only J decreases rapidly upon doping Firpic or $Ir(dmppy)_2(dpp)$ into TCTA. Since FIrpic has the HOMO of 6.15 eV,[32] 0.45 eV deeper than that of TCTA (5.7 eV),[2] the injected holes may collide with the positive barriers and be scattered by these barriers, leading to a reduction of the drift velocity due to an increase of the total transit path.[30] Whereas, upon doping $Ir(dmppy)_2(dpp)$ into TCTA, the J of hole-only device decreases rapidly, which is attributed to the hole trapping effects of $Ir(dmppy)_2(dpp)$ since the HOMO of $Ir(dmppy)_2(dpp)$ (5.05 eV)[33] is higher than that of TCTA (5.7 eV). Hence, the hole mobility is reduced upon doping FIrpic or $Ir(dmppy)_2(dpp)$. Similar phenomenon is obtained by comparing H22 or H23 with H21 because the HOMO of 26DCzPPy (6.05 eV) is lower/higher than that of FIrpic/$Ir(dmppy)_2(dpp)$.[32]

For electron-only devices, the J decreases upon doping FIrpic or $Ir(dmppy)_2(dpp)$ into TCTA, which is attributed to the electron trapping effects of dopants [2] The LUMO of FIrpic (3.47 eV)[32] is much lower than that of TCTA (2.3 eV),[2] resulting in electrons being easily trapped by FIrpic. [2] Although FIrpic is a well-known electron-type dopant,[14] the electron trapping effect by the Firpic reduces the electron transport of E12 compared with that of E11. The electron trapping effect also occurs in $Ir(dmppy)_2(dpp)$ owing to its low LUMO (2.8 eV).[33] On the other hand, electrons are trapped by FIrpic in the 26DCzPPy host since the LUMO of FIrpic is lower than that of 26DCzPPy, resulting in the decreased J in E22. However, the addition of $Ir(dmppy)_2(dpp)$ shows slightly influence on the electron injection and transport in 26DCzPPy by comparing E21 with E23, which is attributed to weak electron trapping effect of $Ir(dmppy)_2(dpp)$ since there is only a 0.05 eV LUMO difference between 26DCzPPy and $Ir(dmppy)_2(dpp)$. Therefore, mobilities of both holes and electrons are reduced upon doping FIrpic or $Ir(dmppy)_2(dpp)$ into the device, leading to the

recombination ratio in the EML being constant with increasing current, which is beneficial to achieving high color-stability and low efficiency roll-off.[2, 30, 31, 37]

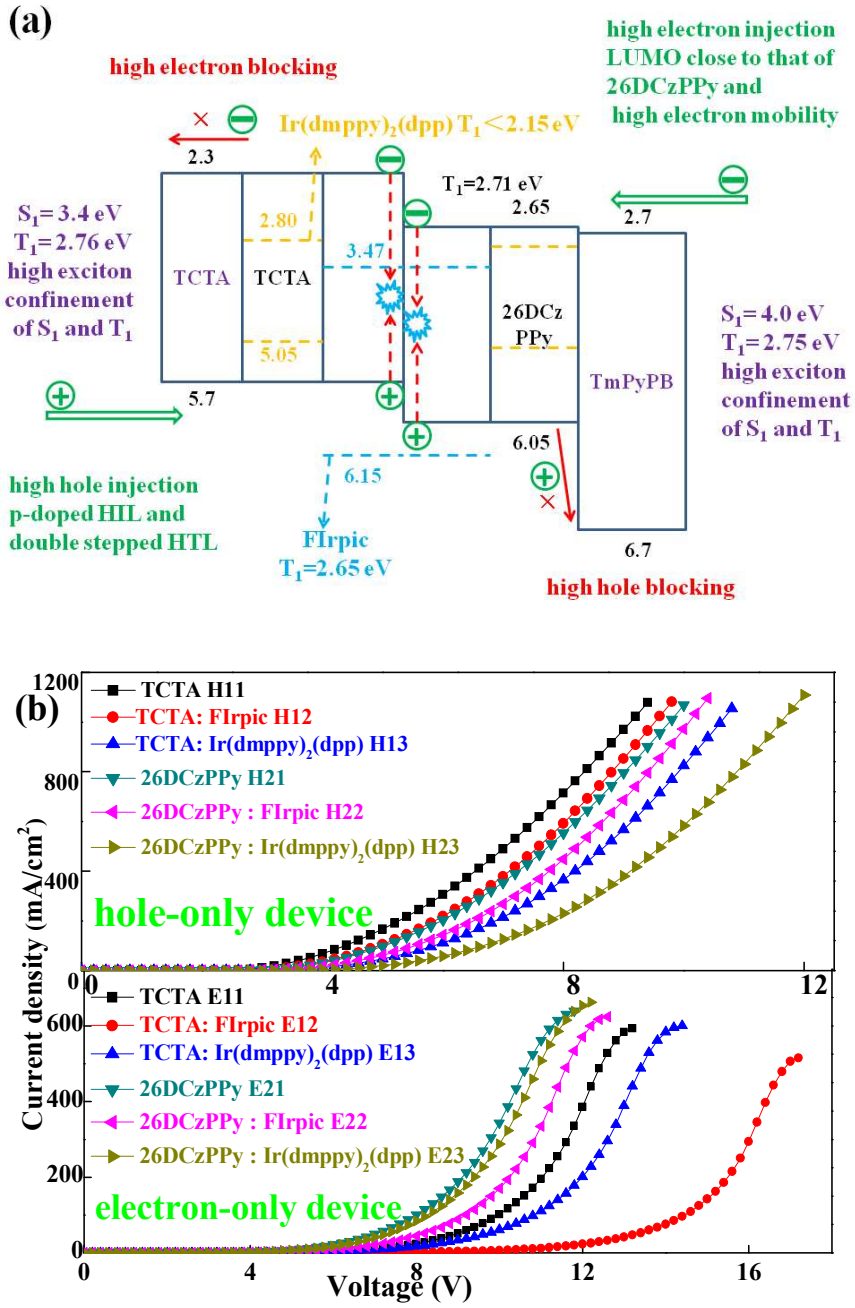

Figure 3. a) A schematic diagram of EL processes and the exciton/charge confinements in W1. b) J-V curves of single-carrier transporting devices.

To further enhance the performance of flexible WOLEDs, we have proposed an inexpensive but effective outcoupling approach by simply dispersing SiO_2 into SU-8 matrix to fabricate

scattering films, extracting the light trapped by the substrate. As shown in figure 4a, more rays (e.g. r2) can be propagated into air via this outcoupling layer due to the well-distributed SiO_2 particles, which demonstrated by the top-viewing (figure 4a3) and cross-sectional (figure 4a4) scanning electron microscopy (SEM) images, leading to an improved factor of ~1.6 during the whole luminance. As displayed in figure 4b and table 1, the resultant device (W2) exhibits a maximum CE and PE of 96.8 cd A^{-1} and 101.3 lm W^{-1} at 4 cd m^{-2}, respectively. At the display-relevant luminance of 100 cd m^{-2}, the CE and PE of 83.8 cd A^{-1} and 77.0 lm W^{-1} are obtained, respectively. At the illumination-relevant luminance of 1000 cd m^{-2}, the CE and PE of 79.1 cd A^{-1} and 58.2 lm W^{-1} are achieved, respectively. More remarkably, W2 shows a nearly unchanged color with the CIE variation of (0.004, 0.005) when the luminance increases from 100 cd m^{-2} to 10000 cd m^{-2}, although the device emits somewhat greenish-white light, as illustrated in figure 4b inset.

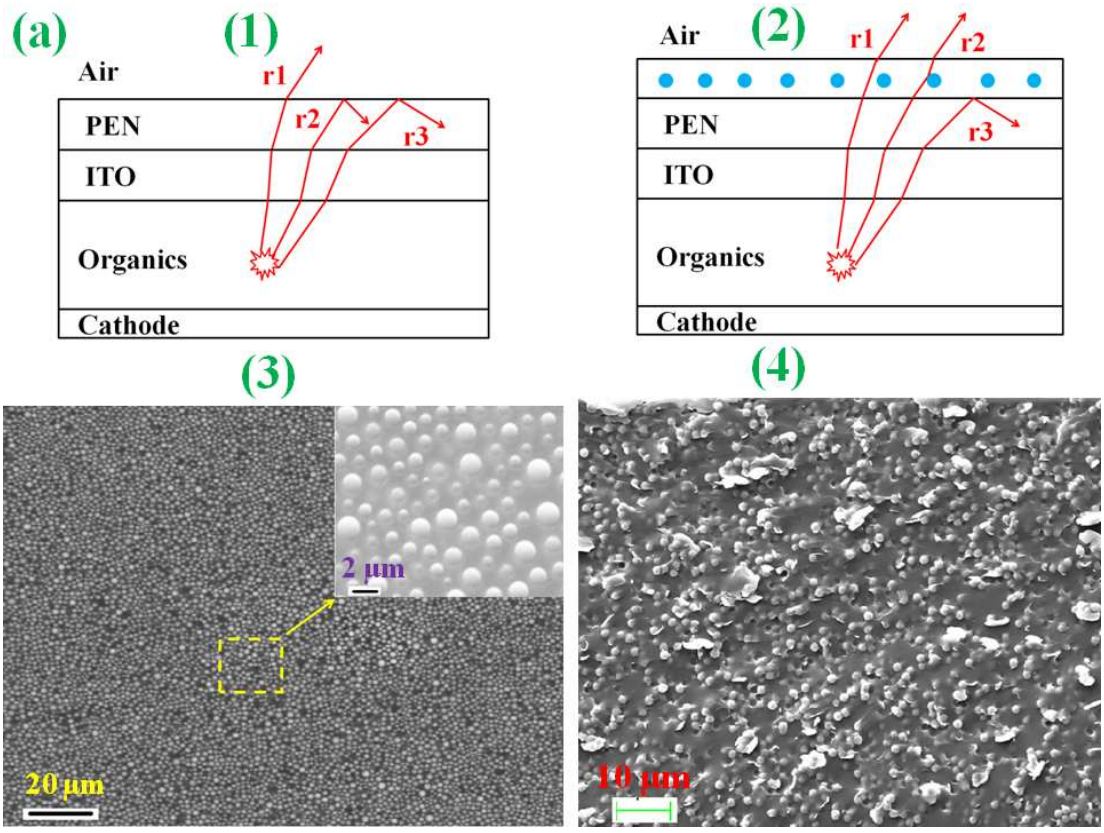

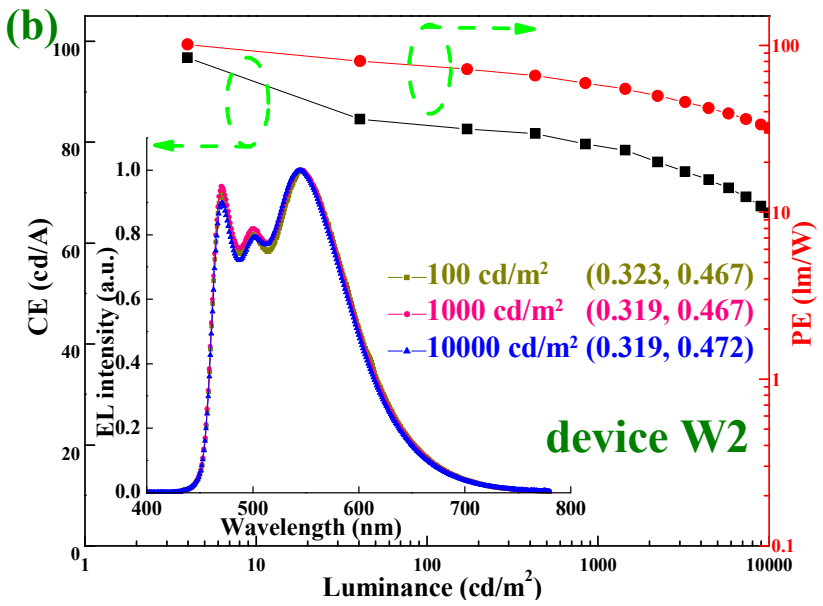

Figure. 4. a) Schematic process of rays propagation without (a1) and with outcoupling layer (a2), SEM images of top-view (a3) and cross-section (a4) for the outcoupling layer. b) Current and power efficiencies as a function of luminance for W2. Inset: EL spectra of W2 at different luminances.

Finally, to further demonstrate the excellent incorporation of mechanical, electrical and optical qualities, a flexible WOLED with 30 × 30 mm emission area is developed (figure 1), implying that our presented schemes are promising for the future large-area applications. It should be pointed out that the presented outcoupling method can also be effectively applied to large-area WOLEDs with glass substrates, demonstrating the universality of this simplified scheme. Besides, two-color WOLEDs exhibit more advantageous than three-color or four-color WOLEDs since they only need two emitting materials, which can vastly lower the cost from the perspective of practical use. But it is deserved to note that the CRI of W2 is not high enough (52 at 1000 cd m^{-2}), which is a common phenomenon in two-color WOLEDs.[2, 14] However, recent studies have demonstrated that two-color WOLEDs can also satisfy the demand of high-quality lighting systems (CRI≥80).[38, 39] Therefore, with the endeavor of materials and chemical scientists, we believe that highly efficient, high CRI associated with low cost flexible WOLEDs can be simultaneously realized if more state-of-the-art

materials were utilized. In addition, although the lifetime of previous flexible WOLEDs has never been reported, it is urged that some lifetime data should be revealed, which is expected to inspire researchers to pay more attention to the lifetime of WOLEDs. As shown in figure 5, the device without thin film encapsulation or outcoupling film (W0), the device with thin film encapsulation but without outcoupling film (W1) and the device with thin film encapsulation and outcoupling film (W2) exhibit a lifetime of 1.7 h, 3.7 h and 5.2 h at an initial luminance of 1000 cd/m^2, respectively. Although the lifetime of W2 is 3 times more than that of W0, W2 is also displays a poor lifetime. This phenomenon can be explained as follows. Since OLEDs are sensitive to the moisture and oxygen, the devices without isolating from the environment by an encapsulation are easily degraded. Therefore, it is reasonable that W0 shows the poorest lifetime among these devices. This analysis can be confirmed by the fact that the lifetime of W1 is 2 times longer than that of W0 via the use of SiNx(300 nm) thin films encapsulation. However, the water vapor transmission rate of this encapsulation is 10^{-3}g/m^2/day, higher than that of ideal encapsulating barriers (10^{-6}g/m^2/day),[40] indicating that much more advanced encapsulation technique can be used to further enhance the lifetime, such as using multilayers fabricated by Al_2O_3 and rapid SiO_2 atomic layer deposition[41] and organic-inorganic multilayer structures[42]. Then, since the outcoupling film can free the light trapped by the substrate, implying that lower voltages can realize the same luminance via the outcoupling film, longer lifetime is obtained for W2. Another important reason for the poor lifetime is ascribed to the well-known fact that FIrpic easily suffers chemical degradation during device operation and an alternative more chemically-stable blue emitter could yield enhanced device lifetimes, although it is still a huge obstacle to date.[43, 44]

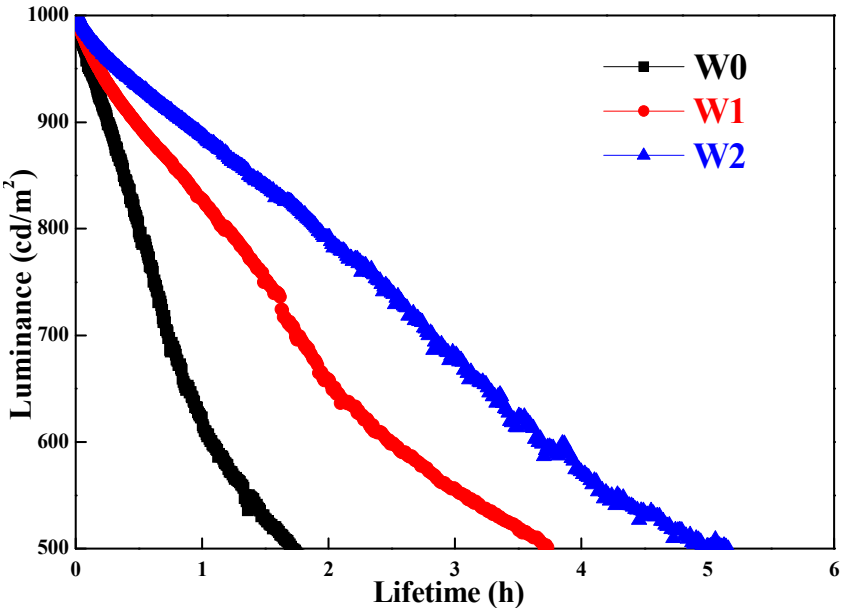

Figure. 5. Luminance decay curves of devices at an initial luminance of 1000 cd/m^2.

4. Conclusion

In summary, we have developed a flexible WOLED with extremely high efficiency and stable color. With the distinguished conjunction of mechanical, electrical and optical properties, the flexible WOLED exhibits a maximum PE of 101.3 lm W^{-1} and 58.2 lm W^{-1} at 1000 cd m^{-2}. Besides, a negligible CIE variation of (0.004, 0.005) during 100- 10000 cd/m^2 is obtained and the origin of the high performance is deeply explored. Such superior results represent a significant step towards extremely high-performance flexible WOLEDs, which will undoubtedly be beneficial to the design of both material and device structure for the commercialization of flexible WOLEDs in the emerging display and lighting applications.

AUTHOR INFORMATION

Corresponding Author

E-mail: zou1007@gmail.com (J. Zou); E-mail: psjbpeng@scut.edu.cn (J. Peng).

Acknowledgments

The authors are grateful to the National Natural Science Foundation of China (Grant Nos.61204087, 61306099, 61401156), the Guangdong Natural Science Foundation (Grant No.

S2012040007003), China Postdoctoral Science Foundation (2014T70835), the Fundamental Research Funds for the Central Universities (2014ZM0003, 2014ZM0034, 2014ZM0037, 2014ZZ0028), Guangdong Innovative Research Team Program (No. 201101C0105067115) and the Specialized Research Fund for the Doctoral Program of Higher Education (Grant No. 20120172120008).

Reference

1 H. Sasabe and J. Kido, *J. Mater. Chem. C*, 2013, **1**, 1699.

2 Q. Wang and D. Ma, *Chem. Soc. Rev.*, 2010, **39**, 2387.

3 F. So and D. Kondakov, *Adv. Mater.* 2010, **22**, 3762.

4 K. T. Kamtekar, A. P. Monkman and M. R. Bryce, *Adv. Mater.* 2010, **22**, 572.

5 G. Gustafsson, Y. Cao, G. M. Treacy, F. Klavetter, N. Colaneri and A. J. Heeger, *Nature* 1992, **357**, 477.

6 G. Gu, P. E. Burrows, S. Venkatesh and S. R. Forrest, *Opt. Lett.* 1997, **22**, 172.

7 Z. B. Wang, M. G. Helander, J. Qiu, D. P. Puzzo, M. T. Greiner, Z. M. Hudson, S. Wang, Z. W. Liu and Z. H. Lu, *Nature Photon.* 2011, **5**, 753.

8 S. Kim, H. Kwon, S. Lee, H. Shim, Y. Chun, W. Choi, J. Kwack, D. Han, M. Song, S. Kim, S. Mohammadi, I. Kee and S. Y. Lee, *Adv. Mater.* 2011, **23**, 3511.

9 E. Najafabadi, K. A. Knauer, W. Haske, C. F. Hernandez and B. Kippelen, *Appl. Phys. Lett.* 2012, **101**, 023304.

10 L. Wang, M. Xu, L. Lan, J. Zou, H. Tao, H. Xu, M. Li, D. Luo and J. Peng, *Scientia Sinica Chimica*, 2013, **43**, 1383.

11 H. Xu, D. Luo, M. Li, M. Xu, J. Zou, H. Tao, L. Lan, L. Wang, J. Peng and Y. Cao, *J. Mater. Chem. C* 2014, **2**, 1255.

12 L. Duan, D. Zhang, K. Wu, X. Huang, L. Wang and Y. Qiu, *Adv. Funct. Mater.* 2011, **21**, 3540.

13 J. H. Jou, S. M. Shen, C. R. Lin, Y. S. Wang, Y. C. Chou, S. Z. Chen and Y. C. Hou, *Org. Electron.* 2011, **12**, 865.

14 S. J. Su, E. Gonmori, H. Sasabe and J. Kido, *Adv. Mater.* 2008, **20**, 4189.

15 H. Sasabe, J. Takamatsu, T. Motoyama, S. Watanabe, G. Wagenblast, N. Langer, O. Molt, E. Fuchs, C. Lennartz and J. Kido, *Adv. Mater.* 2010, **22**, 5003.

16 S. Reineke, F. Lindner, G. Schwartz, N. Sidler, K. Walzer, B. Lussem and K. Leo, *Nature*, 2009, **459**, 234.

17 A. Mikami, T. Koshiy and T. Tsubokawa, *Jpn J. Appl. Phys.* 2005, **44**, 608.

18 J. H. Jou, C. P. Wang, M. H. Wu, H. W. Lin, H. C. Pan and B. H. Liu, *J. Mater. Chem.* 2010, **20**, 6626.

19 W. Ji, J. Zhao, Z. Sun and W. Xie, *Org. Electron.* 2011, **12**, 1137.

20 T. H. Han, Y. Lee, M. R. Choi, S. H. Woo, S. H. Bae, B. H. Hong, J. H. Ahn and T. W. Lee, *Nature Photon.* 2012, **6**, 105.

21 N. Li, S. Oida, G. S. Tulevski, S. J. Han, J. B. Hannon, D. K. Sadana and T. C. Chen, *Nature Commun.* 2013, **4**, 2294.

22 S. Chen, Q. Wu, M. Kong, X. Zhao, Z. Yu, P. Jia and W. Huang, *J. Mater. Chem. C* 2013, **1**, 3508.

23 K. R. Sarma, J. Roush, J. Schmidt, C. Chanley, S. Dodd, *Proc. of ASID*, 2006, 337.

24 B. O'Brien, Y. K. Lee, M. Marrs, J. Smith, M. Strnad, E. Forsythe and D. Morton, *SID Digest*, 2013, 447.

25 Q. Wang, J. Ding, D. Ma, Y. Cheng, L. Wang, X. Jing and F. Wang, *Adv. Funct. Mater.* 2009, **19**, 84.

26 S. Gong, Y. Chen, J. Luo, C. Yang, C. Zhong, J. Qin and D. Ma, *Adv. Funct. Mater.* 2011, **21**, 1168.

27 J. Ye, C. Zheng, X. Ou, X. Zhang, M. Fung and C. Lee, *Adv. Mater.* 2012, **24**, 3410.

28 B. Pan, B. Wang, Y. Wang, P. Xu, L. Wang, J. Chen and D. Ma, *J. Mater. Chem. C* 2014, **2**, 2466.

29 Q. Wang, J. Ding, D. Ma, Y. Cheng and L.Wang, *Appl. Phys. Lett.*, 2009, **94**, 103503.

30 Y. S. Park, J. W. Kang, J. W. Park, Y. H. Kim, S. K. Kwon, and J. J. Kim, *Adv. Mater.* 2008, **20**, 1957.

31 B. Liu, L. Wang, M. Xu, H. Tao, X. Xia, J. Zou, Y. Su, D. Gao, L. Lan and J. Peng, *J. Mater. Chem. C* 2014, **2**, 5870.

32 C. Cai, S. J. Su, T. Chiba, H. Sasabe, Y. J. Pu, K. Nakayama and J. Kido, *Org. Electron.* 2011, **12**, 843.

33 http://www.lumtec.com.tw.

34 G. He, M. Pfeiffer, K. Leo, M. Hofmann, J. Birnstock, R. Pudzich and J. Salbeck, *Appl. Phys. Lett.*, 2004, **85**, 3911.

35 C. Diez, T. C. G. Reusch, S. Seidel and W. Brutting, *J. Appl. Phys.* 2012, **111**, 113102.

36 S. J. Su, T. Chiba, T. Takeda and J. Kido, *Adv. Mater.* 2008, **20**, 2125.

37 Q. Wang, C. L. Ho, Y. Zhao, D. Ma, W. Y. Wong and L. Wang, *Org. Electron.* 2010, **11**, 238.

38 B. Yan, C. C. C. Cheung, S. C. F. Kui, H. Xiang, V. A. L. Roy, S. Xu and C. Che, *Adv. Mater.* 2007, **19**, 3599.

39 C. H. Chang, C. C. Chen, C. C. Wu, S. Y. Chang, J. Y. Hung and Y. Chi, *Org. Electron.* 2010, **11**, 266.

40 J. S. Park, H. Chae, H. K. Chung and S. I. Lee, *Semicond. Sci. Technol*. 2011, **26**, 034001.

41 A. A. Dameron, S. D. Davidson, B. B. Burton, P. F. Carcia, R. S. Mclean and S. M. George, *J. Phys. Chem. C* 2008, **112**, 4573.

42 S. W. Seo, E. Jung, S. J. Seo, H. Chae, H. K. Chung and S. M. Cho, *J. Appl. Phys.* 2013, **114**, 143505.

43 V. Sivasubramaniam, F. Brodkorb, S. Hanning, H. P. Loebl, V. V. Elsbergen, H. Boerner, U. Scherf and M. Kreyenschmidt, *J. Fluorine Chem.* 2009, **130**, 640.

44 V. N. Kozhevnikov, Y. Zheng, M. Clough, H. A. Al-Attar, G. C. Griffiths, K. Abdullah, S. Raisys, V. Jankus, M. R. Bryce and A. P. Monkman, *Chem. Mater.* 2013, **25**, 2352.

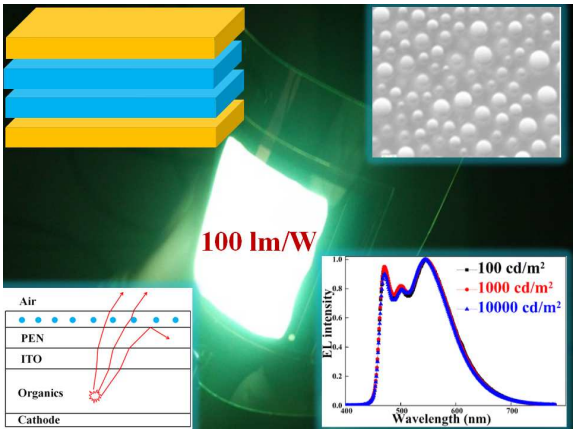

Flexible WOLEDs with extreme efficiency and color-stability are realized via the extraordinary combination of mechanical, electrical and optical properties.